

UC Riverside

UC Riverside Electronic Theses and Dissertations

Title

Effects of Experimental Nitrogen Deposition on Dryland Soil Organic Carbon Storage

Permalink

<https://escholarship.org/uc/item/8c0536rb>

Author

Puespoek, Johann Ferenc

Publication Date

2022

Supplemental Material

<https://escholarship.org/uc/item/8c0536rb#supplemental>

Peer reviewed|Thesis/dissertation

UNIVERSITY OF CALIFORNIA
RIVERSIDE

Effects of Experimental Nitrogen Deposition on Dryland Soil Organic Carbon Storage

A Thesis submitted in partial satisfaction
of the requirements for the degree of

Master of Science

in

Environmental Sciences

by

Johann Ferenc Puespoek

March 2022

Thesis Committee:

Dr. Peter M. Homyak, Chairperson

Dr. Samantha C. Ying

Dr. Francesca M. Hopkins

Copyright by
Johann Ferenc Puespoek
2022

The Thesis of Johann Ferenc Puespoek is approved:

Committee Chairperson

University of California, Riverside

Acknowledgments

I would like to thank the Homyak lab for being such a fun environment to work in. Thank you, Aral Greene, Elizah Stephens, Tony Calma, Sharon Zhao, Alex Krichels and Pete Homyak. A special thanks to Pete Homyak for being such a patient and understanding advisor in good and bad times. I would also like to thank Francesca Hopkins and Samantha Ying for being on my committee and providing such great feedback. Thank you, Nathan Sy, for helping me with the freeze-dryer. Thank you, Ying Lin, for analyzing my soil samples on the EA-IRMS. Thank you, David Lyons, for all the help with analyzing samples and showing me how to use all those instruments in the analytical lab. Huge thanks to George Vourlitis and Steven Allison for collaborating with me and letting me use their experimental sites. Thank you to all my friends and family from back home for the unconditional support no matter where I am in the world. But most importantly, a huge thank you to all the new friends I made during my time in Riverside.

ABSTRACT OF THE THESIS

Effects of Experimental Nitrogen Deposition on Dryland Soil Organic Carbon Storage

by

Johann Ferenc Puespoek

Master of Science, Graduate Program in Environmental Sciences
University of California, Riverside, March 2022
Dr. Peter M. Homyak, Chairperson

Nitrogen enrichment due to atmospheric nitrogen deposition has affected plant growth and microbial activity globally, leading to an increase in soil organic carbon in many ecosystems. Drylands cover ~45% of the global land area and store ~32% of the global carbon stocks, but the response of dryland carbon storage to atmospheric nitrogen deposition remains unclear and understudied relative to mesic systems. To help identify changes in carbon storage, soil organic carbon can be separated into a plant-derived, particulate organic carbon fraction, and a largely microbially-derived, mineral-associated organic carbon fraction. Observations from mesic systems suggest that nitrogen enrichment should increase the efficiency by which microbes incorporate carbon into mineral-associated forms (carbon stabilization efficiency) if pH stays constant. Under acidification, a common response to nitrogen deposition—microbial biomass and enzymatic organic matter decay should decrease, leading to a build-up in particulate

organic carbon. However, in drylands, where organic carbon often associates with mineral surfaces via Ca-bridging, acidification can also abiotically affect mineral-associated organic carbon if Ca is leached. To test how nitrogen deposition affects dryland carbon storage I used four long-running experimental nitrogen deposition experiments in Southern California, where two of the sites showed strong nitrogen-induced acidification. I studied changes in soil organic carbon fractions, soil extracellular enzyme activities, microbial carbon stabilization efficiency and exchangeable Ca. Experimental nitrogen deposition had relatively small effects on soil organic carbon storage, which appeared to be mostly driven by soil physicochemical changes. Particulate organic carbon did not increase despite previously reported increases in plant biomass, and decreases in microbial biomass and extracellular enzyme activities in acidified sites. Furthermore, microbial carbon stabilization efficiency was unaffected by N fertilization in non-acidified sites, but decreased in short-term but not long-term incubations in acidified sites. Importantly, mineral-associated organic carbon decreased significantly at one of the acidified sites, likely as result of pH-induced Ca loss. Our measurements suggest that long-term effects of nitrogen fertilization on dryland carbon storage might be of abiotic nature, such that drylands where Ca-stabilization of soil organic carbon is prevalent and may undergo acidification, may be most at risk for significant loss of mineral-associated organic carbon.

TABLE OF CONTENTS

| | |
|---|----|
| INTRODUCTION..... | 1 |
| MATERIAL AND METHODS | 6 |
| Site description..... | 6 |
| Soil sampling | 8 |
| Microbial biomass C and N | 9 |
| Soil hydrolytic enzyme activities | 10 |
| Soil organic matter fractionation | 11 |
| Carbon stabilization efficiency..... | 12 |
| Calculations and statistical analyses | 13 |
| RESULTS | 15 |
| Soil organic C fractions | 15 |
| Microbial biomass and potential extracellular enzyme activities | 17 |
| Carbon stabilization efficiency and exchangeable Ca | 19 |
| DISCUSSION..... | 21 |
| Microbial C stabilization efficiency..... | 24 |
| Mineral-associated organic C | 25 |
| Implications for N deposition effects on C storage in drylands | 27 |
| REFERENCES..... | 29 |

LIST OF FIGURES

- Figure 1.** Conceptual overview over the processes that contribute to soil organic C (SOC) formation as particulate organic C (POC) and mineral-associated organic C (MAOC).4
- Figure 2.** Differences in particulate organic C between control plots and plots fertilized with N during the wet season 2021 in soils from four long-term (> 10 years) N fertilization experiments in Southern California. At Chaparral and Coastal sage scrub 1 soils are from beneath shrubs and from interspaces between shrubs and at Grassland and Coastal sage scrub 2 soils are from beneath vegetation only. Chaparral and Coastal sage scrub 1 experienced strong acidification in response to N fertilization. Dots represent individual data points (4 plots per treatment and soil position) with grey lines connecting paired control and N-fertilized plots. Black crossbars represent means (n=4). If present, significant N fertilization effects across the beneath shrub and interspace samples are given in inset box (two-way ANOVA), and significant N fertilization effects within soil positions (paired t-test) are indicated by symbols above data points (*, p<0.1, **, p<0.05).....16
- Figure 3.** Differences in mineral-associated organic C between control plots and plots fertilized with N during the wet season 2021 in soils from four long-term (> 10 years) N fertilization experiments in Southern California. At Chaparral and Coastal sage scrub 1 soils are from beneath shrubs and from interspaces between shrubs and at Grassland and Coastal sage scrub 2 soils are from beneath vegetation only. Chaparral and Coastal sage scrub 1 experienced strong acidification in response to N fertilization. Dots represent individual data points (4 plots per treatment and soil position) with grey lines connecting paired control and N-fertilized plots. Black crossbars represent means (n=4). If present, significant N fertilization effects across beneath shrub and interspace samples are given in inset box (Two-way ANOVA), and significant N fertilization effects within soil positions (paired t-test) are indicated by symbols above data points (*, p<0.1, **, p<0.05).....17
- Figure 4.** Differences in microbial biomass C between control plots and plots fertilized with N during the wet season 2021 in soils from four long-term (> 10 years) N fertilization experiments in Southern California. At Chaparral and Coastal sage scrub 1 soils are from beneath shrubs and from interspaces between shrubs and at Grassland and Coastal sage scrub 2 soils are from beneath vegetation only. Chaparral and Coastal sage scrub 1 experienced strong acidification in response to N fertilization. Dots represent individual data points (4 plots per treatment and soil position) with grey lines connecting paired control and N-fertilized plots. Black crossbars represent means (n=4). If present, significant N fertilization effects across soil position (beneath shrub and interspace) samples are given in inset box (two-way ANOVA), and significant N fertilization effects within soil positions (paired t-test) are indicated by symbols above data points (*, p<0.1, **, p<0.05).18
- Figure 5.** Differences in carbon stabilization efficiency measured in short- (1 day; i.e. community-scale carbon stabilization efficiency (CSE_c)) and long-term (2 weeks; i.e. ecosystem-scale carbon stabilization efficiency (CSE_E)) incubations between control plots and plots fertilized with N during the wet season 2021 in soils from four long-term (> 10 years) N fertilization experiments in Southern California. Chaparral and Coastal

sage scrub 1 experienced strong acidification in response to N fertilization. Dots represent individual data points (4 plots per treatment and soil position) with grey lines connecting paired control and N-fertilized plots. Black crossbars represent means (n=4). If present, significant N fertilization effects within each incubation time (paired t-test) are indicated by symbols above data points (*, p<0.1, **, p<0.05).....20

Figure 6. Differences in exchangeable Ca between control plots and plots fertilized with N during the wet season 2021 in soils from four long-term (> 10 years) N fertilization experiments in Southern California. At Chaparral and Coastal sage scrub 1 soils are from beneath shrubs and from interspaces between shrubs and at Grassland and Coastal sage scrub 2 soils are from beneath vegetation only. Chaparral and Coastal sage scrub 1 experienced strong acidification in response to N fertilization. Dots represent individual data points (4 plots per treatment and soil position) with grey lines connecting paired control and N-fertilized plots. Black crossbars represent means (n=4). If present, significant N fertilization effects across beneath shrub and interspace samples are given in inset box (two-way ANOVA), and significant N fertilization effects within soil positions (paired t-test) are indicated by symbols above data points (*, p<0.1, **, p<0.05).....21

LIST OF TABLES

| | |
|---|----|
| Table 1. Soil characteristics. Data are means (standard deviation; n=4). Numbers in bold indicate significant differences between control plots and plots fertilized with N evaluated in a two-way ANOVA across soil positions for CHAP and CSS1 and in paired t-tests for GRASS and CSS2 (p<0.1). | 7 |
| Table 2. Water-extractable organic C (WEOC), water-extractable organic C to N ration (WEO C:N), extractable ammonium (NH ₄ ⁺) and extractable nitrate (NO ₃ ⁻). Data are means (standard deviation; n=4). Numbers in bold indicate significant differences between control plots and plots fertilized with N evaluated in a Two-way ANOVA across soil positions for CHAP and CSS1 and in paired t-tests for GRASS and CSS2 (p<0.1).... | 8 |
| Table 3. Soil extracellular enzymes measured and their abbreviations and functions. | 11 |
| Table 4. Potential activities of C-acquiring soil extracellular enzymes alpha-glucosidase (AG), beta-glucosidase (BG) and cellobiohydrolase (CBH) and N-acquiring soil extracellular enzymes N-acetyl-glucosaminidase (NAG) and leucine-aminopeptidase (LAP). Data are means (standard deviation). Numbers in bold indicate significant differences between control plots and plots fertilized with N evaluated in a two-way ANOVA across soil positions for CHAP and CSS1 and in paired t-tests for GRASS and CSS2 (p<0.1)..... | 19 |

INTRODUCTION

Atmospheric nitrogen (N) deposition has tripled since 1850, due to emissions from agriculture and fossil fuel burning, leading to a global enrichment of soil N pools (Gruber and Galloway 2008; Kanakidou et al. 2016). This N enrichment affects plant growth and microbial activity and thereby strongly interacts with the global carbon (C) cycle (Gruber and Galloway 2008; Treseder 2008; O'Sullivan et al. 2019). Soil organic carbon (SOC) contains more C than vegetation and the atmosphere combined and confers important soil functions such as soil fertility and water retention (Weil and Brady 2017). Globally, SOC pools have increased by 4.2% in response to N enrichment (Xu et al. 2021), but responses can be biome-specific (Deng et al. 2020). Drylands make up ~45% of the global land area and store up to 32% of the global C stocks (Právělie 2016; Plaza et al. 2018b). Therefore, dryland response to N deposition could have substantial consequences on global C cycling and soil quality (Homyak et al. 2014; Plaza et al. 2018a), but they are underrepresented in global analyses evaluating N fertilization effects on soil C storage (Xu et al. 2021). While both increases and decreases in SOC have been measured along N deposition gradients (Ochoa-hueso et al. 2013; Maestre et al. 2016), the magnitude of and mechanisms behind dryland C storage change in response to N deposition remain unclear. The effects of N deposition on dryland SOC storage depend on many factors including changes in plant C inputs, organic matter decomposition, microbial transformations of C compounds, and stabilization of C in soil minerals. To help identify changes in SOC storage and the mechanisms governing the fate of C in response to N deposition, SOC can be separated into pools of different origin and persistence (Lavallee et al. 2020). Soil organic C can be broadly separated into a relatively faster cycling, particulate organic C (POC) fraction, consisting of relatively undecomposed plant material, and a relatively slower cycling, mineral-associated organic C (MAOC) fraction, consisting of heavily decomposed plant compounds and microbial products

(Lavallee et al. 2020). Due to their differences in formation, the largely plant-derived POC should depend mostly on N-induced changes in plant biomass production and decomposition (Rossi et al. 2020), while changes in MAOC should depend more strongly on litter quality, microbial metabolism, and soil sorption potential (Fig. 1) (Castellano et al. 2015; Sokol et al. 2019). Separating SOC into POC and MAOC revealed that N fertilization effects on C storage in semi-arid grasslands were mostly driven by increased aboveground biomass and POC, but microbial C cycling and mineral stabilization in the MAOC pool may be also important (Ye et al. 2018; Lin et al. 2019).

In particular, an important pathway for MAOC build-up is thought to involve the in-vivo transformation of C compounds – also known as the “microbial C pump” into microbial biomass and microbial by-products (Liang et al. 2017). Carbon that cycles through the “pump” can then associate with mineral surfaces upon microbial death or exudation where it becomes protected from decomposition. Therefore, microbial C use efficiency (CUE), the efficiency by which microbes retain C in their biomass vs. C they respire, is key to determining SOC storage (Bradford et al. 2013). Microbial CUE is frequently measured by tracing microbial incorporation and respiration of isotopically-labelled C compounds and depends on many factors such as community composition, climate, soil physicochemical conditions and nutrient status (Manzoni et al. 2012a; Jones et al. 2019; Butcher et al. 2020; Pold et al. 2020). Microbial carbon stabilization efficiency (CSE) extends the CUE term by accounting for the formation of microbial residues that can be stabilized in soil, and can thus link N-induced changes in microbial physiology with long-term C stabilization, particularly when measured over longer time periods (e.g., multiple weeks) (Geyer et al. 2020). Previous studies in temperate grasslands found that adding N increased CUE and SOC storage (Poepflau et al. 2019). However, in drylands, microbes may be limited by C or there may be no link between CUE and MAOC formation due to the low sorption potential of

coarse dryland soils (Schaeffer et al. 2003; Creamer et al. 2014, 2016; Cai et al. 2022). How microbial CSE or CUE change in response to N enrichment has not been measured before in drylands, and it is not known whether N deposition will affect C storage via changes in the microbial C pump.

The effects of atmospheric N deposition on SOC may also be confounded by site-specific factors under the control of N enrichment. For example, models suggest N enrichment should favor the transformation of POC into persistent MAOC, so as long as decomposition is N limited and soils do not become too acidic to adversely affect microbial physiology (Averill and Waring 2018). However, acidification is a common consequence of N enrichment resulting from H^+ release in nitrification, H^+ release after plants take up NH_4^+ , and leaching of base cations as companion ions to NO_3^- (Tian and Niu 2015). Thus, many studies actually attribute increases in SOC after N enrichment to acidity-induced decreases in microbial biomass and decreased organic matter decomposition leading to a build-up of POC without producing MAOC (Treseder 2008; Janssens et al. 2010; Riggs and Hobbie 2016; O'Sullivan et al. 2019). Identifying which mechanism governs SOC dynamics has, therefore, been challenging, especially because drylands can be well-buffered against changes in pH (Slessarev et al. 2016), potentially protecting microbes from acidification. Because decomposition is largely driven by enzymes that break down polymers into smaller, more easily assimilated compounds (Burns et al. 2013), extracellular enzyme activities may offer an opportunity to disentangle whether acidification affects microbial decomposition, the partitioning of C, and the fate of both POC and MAOC pools.

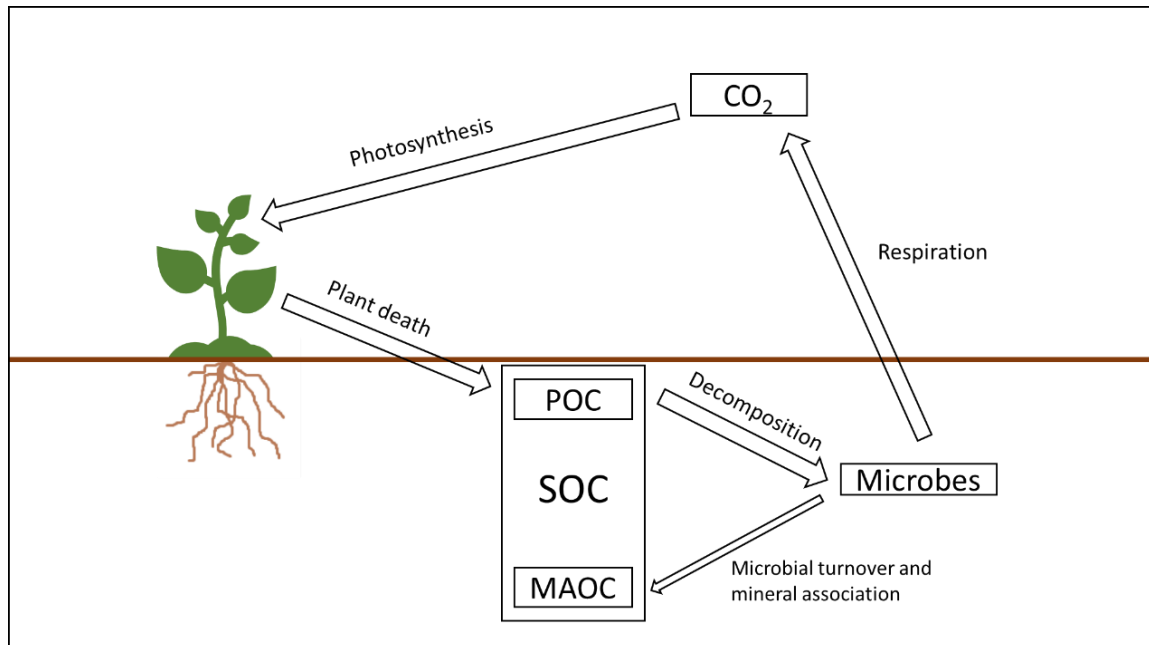


Figure 1. Conceptual overview over the processes that contribute to soil organic C (SOC) formation as particulate organic C (POC) and mineral-associated organic C (MAOC).

Besides the direct effects of acidification on microbial physiology and ensuing effects on POC and MAOC pools, MAOC may also be altered directly via soil physicochemical changes. The amount of MAOC that can be stabilized in soil depends on the availability of soil sorption sites (Castellano et al. 2015; Cotrufo et al. 2019). In dryland soils, SOC stabilization is thought to be primarily controlled by clay content and exchangeable calcium (Ca) (Rasmussen et al. 2018). Polyvalent cations like Ca can stabilize SOC by bridging negatively charged C compounds with negatively charged mineral surfaces or by binding together multiple organic molecules (Rowley et al. 2018). There is evidence that N enrichment can destabilize Ca-bridges and MAOC via leaching losses of Ca due to acidification (Ye et al. 2018; Wan et al. 2021), but it is unclear how widespread such pH-induced MAOC losses are in relatively well-buffered drylands.

To understand how N fertilization and changes in soil physicochemical properties may impact SOC storage and cycling, N fertilization experiments offer unique opportunities to simulate the

effects of atmospheric N deposition by adding known amounts of N to ecosystems in controlled, experimental settings. These controlled experiments reduce the natural variation in confounding factors often present in studies along natural gradients and are routinely used to directly study N-enrichment effects on ecosystems. In this study, I take advantage of multiple long-running (i.e., > 14 years) N fertilization experiments in Southern California that include four sites across dominant dryland ecosystems: One grassland site, two sites in deciduous shrub-dominated coastal sage scrub (CSS) and one site in evergreen shrub-dominated chaparral. The sites differed in their response to N addition, with two of the shrublands showing strong acidification, allowing me to study how site-specific responses may differently affect SOC fractions. Specifically, I ask:

- 1) How does long-term N fertilization affect C storage in POC and MAOC pools in dryland ecosystems?
- 2) Does dryland N fertilization change the stabilization efficiency of labile C inputs via the microbial C pump?

To answer these questions, I used a combination of size and density fractionation to separate soils from the four dryland N fertilization sites into POC and MAOC pools. To explore which mechanisms may control changes in soil C fractions, I measured changes in exchangeable Ca as proxy for how C stabilization potential was affected by N fertilization, and microbial biomass and enzyme activities as proxies for how microbial decomposition was affected by N fertilization. Furthermore, I assessed carbon stabilization efficiency (CSE) by measuring the efficiency by which microbes retained ^{13}C -labelled glucose in soil in both short- and long-term incubations. I hypothesized that a) the previously reported increase in above-ground biomass in response to N addition at three of the sites (Parolari et al. 2012; Vourlitis et al. 2021a) would lead to an increase in POC, particularly in acidified plots where decomposition might be inhibited; b) alleviation of

N limitation would increase CSE and transformation of POC into MAOC in non-acidified plots; and c) N fertilization would decrease exchangeable Ca and MAOC in acidified plots.

MATERIAL AND METHODS

Site description

The study was conducted at three long-running N fertilization experiments in Southern California that together consist of four sites and represent the three dominant vegetation systems in the region (chaparral, CSS, and grassland). The chaparral site (CHAP) is located at the Sky Oaks Field Station in San Diego County, CA (33.381 N, 116.626 W, elev. 1420 m). The first CSS site (CSS1) is located at Santa Margarita Ecological Reserve in Riverside County, CA (33.438 N, 117.181 W, elev. 248 m). The grassland site (GRASS) and second CSS site (CSS2) are part of the Loma Ridge Global Change Experiment located at Irvine Ranch National Landmark in Orange County, California (33.742 N, 117.704 W, elev. 365 m). All sites experience Mediterranean climate with cool, wet winters and hot, dry summer with most of the rain falling between November and April.

CHAP and CSS1 are extensively described in Vourlitis et al. (2021). Mean annual precipitation at CHAP is 382 mm. Vegetation is dominated by *Adenostoma fasciculatum* and *Ceanothus greggii*. Soils are Ultic Haploxerolls (Sheephead series) derived from micaceous shist and have a sandy loam texture. The site burned at the onset of the experiment in 2003. CHAP experienced severe acidification in response to N fertilization, with soil pH in N-fertilized plots being 1.65 pH units below control plots in 2021 (Table 1). Mean annual precipitation at CSS1 is 414 mm. Vegetation is dominated by *Artemisia californica* and *Salvia mellifera*. Soils are Typic Rhodoxeralfs formed from weathered Gabbro material (Las Posas series) and have a sandy clay loam texture. CSS1 experienced severe acidification in response to N fertilization, with soil pH in N-fertilized plots being 1.49 pH units below control plots in 2021 (Table 1). CHAP and CSS1 have the same

experimental layout, consisting of 8 plots in 4 pairs. Each pair consists of one 10 x 10 m control plot and one 10 x 10 m fertilized plot. Plots have been fertilized with 50 kgN ha⁻¹ y⁻¹ each fall since 2003 as either NH₄NO₃ (2003–07), (NH₄)₂SO₄ (2007–09), or urea (2009-present). Background N deposition rate at both sites is estimated as 2-4 kgN ha⁻¹ y⁻¹ (Fenn et al. 2010).

Table 1. Soil characteristics. Data are means (standard deviation; n=4). Numbers in bold indicate significant differences between control plots and plots fertilized with N evaluated in a two-way ANOVA across soil positions for CHAP and CSS1 and in paired t-tests for GRASS and CSS2 (p<0.1).

| | | Soil pH | | Sand fraction C (mg g ⁻¹) | | Soil organic C (mg g ⁻¹) | | Soil organic N (mg g ⁻¹) | | Soil organic C:N | |
|-------|------------|----------------|------------------------------|---------------------------------------|----------------|--------------------------------------|-------------------------------|--------------------------------------|------------------------------|------------------|-------------------------------|
| | | Control | N added | Control | N added | Control | N added | Control | N added | Control | N added |
| CHAP | Shrub | 6.64 (0.35) | 4.90 (0.11) | 1.98 (0.26) | 1.77 (0.23) | 15.90 (4.07) | 13.44 (3.59) | 0.65 (0.20) | 0.63 (0.19) | 29.44 (4.19) | 24.97 (1.78) |
| | Interspace | 6.63 (0.26) | 5.07 (0.25) | 1.98 (0.31) | 1.91 (0.41) | 13.03 (3.91) | 8.68 (0.56) | 0.61 (0.29) | 0.39 (0.09) | 27.68 (5.58) | 27.37 (5.28) |
| CSS1 | Shrub | 6.53 (0.19) | 5.20 (0.46) | 0.74 (0.34) | 0.54 (0.09) | 16.17 (4.88) | 11.89 (3.08) | 1.16 (0.35) | 0.97 (0.31) | 16.30 (1.19) | 14.51 (1.17) |
| | Interspace | 6.82 (0.25) | 5.17 (0.13) | 0.50 (0.07) | 0.58 (0.21) | 11.73 (4.78) | 12.50 (3.39) | 0.82 (0.32) | 0.99 (0.32) | 16.51 (0.58) | 15.01 (1.63) |
| GRASS | | 6.55 (0.36) | 6.61 (0.20) | 0.68 (0.07) | 0.57 (0.06) | 14.78 (2.20) | 15.37 (3.22) | 1.22 (0.15) | 1.29 (0.26) | 14.11 (0.71) | 13.89 (0.47) |
| CSS2 | | 6.31 (0.23) | 6.58 (0.17) | 0.80 (0.17) | 0.95 (0.17) | 13.65 (1.02) | 13.69 (2.37) | 1.22 (0.11) | 1.25 (0.23) | 13.11 (0.45) | 12.79 (0.32) |

Vegetation at the Loma Ridge Global Change Experiment is a mosaic of non-native annual grassland and CSS and hosts the GRASS and CSS2 sites. Mean annual precipitation is 281 mm (Khalili et al., 2016). Vegetation at GRASS can vary but typically includes *Bromus diandrus*, *Lolium multiflorum* and *Avena fatua*. Abundant species at CSS2 include *Malosma laurina*, *Artemisia californica* and *Salvia mellifera* (Potts et al., 2012). Soils are Typic Palexeralfs (Myford series) formed on colluvial deposits formed from sedimentary rocks and have a sandy loam texture (Khalili et al. 2016). GRASS and CSS2 have the same randomized split-plot design, consisting of 4 replicate plots that are split into an unfertilized half and a half fertilized with 60 kgN ha⁻¹ y⁻¹. Plots have been fertilized since 2007 with 20 kgN ha⁻¹ y⁻¹ as immediate-release CaNO₃ prior to the wet season and 40 kgN ha⁻¹ y⁻¹ as 100-day release CaNO₃ during the wet

season. Background N deposition rate is estimated as 15 kgN ha⁻¹ y⁻¹ (Fenn et al. 2010). The plots burned when fertilization started in 2007 and again in November 2020.

Table 2. Water-extractable organic C (WEOC), water-extractable organic C to N ratio (WEO C:N), extractable ammonium (NH₄⁺) and extractable nitrate (NO₃⁻). Data are means (standard deviation; n=4). Numbers in bold indicate significant differences between control plots and plots fertilized with N evaluated in a Two-way ANOVA across soil positions for CHAP and CSS1 and in paired t-tests for GRASS and CSS2 (p<0.1).

| | | WEOC (µg g ⁻¹) | | WEO C:N | | NH ₄ ⁺ (µg g ⁻¹) | | NO ₃ ⁻ (µg g ⁻¹) | |
|-------|------------|----------------------------|-------------------|-----------------|------------------------------|--|------------------------------|--|--------------------------------|
| | | Control | N added | Control | N added | Control | N added | Control | N added |
| CHAP | Shrub | 37.94 (7.24) | 51.08 (25.62) | 13.87 (4.24) | 4.69 (2.97) | 0.40 (0.21) | 6.90 (4.22) | 0.06 (0.10) | 12.72 (5.84) |
| | Interspace | 20.25 (8.58) | 17.84 (5.80) | 17.79 (5.02) | 4.50 (4.06) | 0.45 (0.29) | 9.04 (8.44) | 0.06 (0.08) | 7.27 (4.61) |
| CSS1 | Shrub | 85.47 (23.95) | 124.73 (62.75) | 17.81 (5.37) | 5.54 (3.16) | 0.81 (0.27) | 6.92 (4.50) | 0.76 (0.55) | 19.43 (10.80) |
| | Interspace | 83.10 (21.17) | 91.70 (30.06) | 12.10 (4.46) | 1.86 (0.21) | 1.70 (1.08) | 3.19 (2.18) | 3.83 (4.80) | 42.42 (10.97) |
| GRASS | | 83.79 (22.43) | 74.20 (12.55) | 10.84 (3.70) | 4.40 (1.42) | 1.79 (0.70) | 2.37 (0.70) | 3.77 (2.21) | 14.22 (5.14) |
| CSS2 | | 81.63 (4.71) | 137.57 (95.55) | 13.78 (1.11) | 8.70 (2.56) | 0.97 (0.22) | 1.50 (0.25) | 0.56 (0.23) | 3.39 (1.00) |

Soil sampling

Soil samples were taken at the end of the dry season in October 2020 and at the end of the wet season in April 2021. After removing plant litter from the soil surface, two sub-samples of soil were taken from each plot and combined into one composite sample using a soil auger (2.54 cm diameter x 10 cm depth). Soil samples were taken from randomly selected locations in the grassland plots and from underneath randomly selected shrubs in the chaparral and CSS plots. At Sky Oaks and Santa Margarita additional soil samples were taken from the interspaces between shrubs, yielding one “Beneath shrub” and one “Interspace” sample per plot. No interspace samples were taken at Loma Ridge since there was no significant area of bare soil. Soil samples were brought back to the Environmental Sciences department at UC Riverside and sieved to 2 mm for all further lab analysis. Field-moist soil samples were kept at 4°C. All measurements on

field-moist soil samples were done within one week of sampling to reduce storage effects.

Gravimetric water content was measured by drying field-moist soil samples at 105°C for 24h. All data reported is expressed on a per g dry weight basis.

Total C and N, soil pH, exchangeable Ca^{2+} , exchangeable NO_3^- and NH_4^+ and water-extractable organic C

Total C and N content of air-dried, ground soil samples were measured after combustion using a FlashEA 1112 NC analyzer (Thermo Fisher Scientific Inc., Waltham, MA). Soil pH was measured with a glass electrode on air-dried soil in nanopure water (1:2 (w:v) soil dry weight:solution). Exchangeable Ca^{2+} was measured in 0.1 M BaCl_2 extracts of air-dried soil ((1:20) soil dry weight:solution) by inductively-coupled plasma optical-emission spectrometry (ICP-OES) using an Optima 7300 DV (Perkin-Elmer Inc., Shelton, CT) (Hendershot and Duquette 1986). Exchangeable nitrate (NO_3^-) and ammonium (NH_4^+) were measured in 2 M KCl extracts of field-moist soil (1:10 (w:v) soil dry weight:solution) on an AQ2 Discrete Analyzer (SEAL Analytical, Mequon, WI). Water-extractable organic C (=WEOC) was measured in nanopure water extracts of field-moist soil (1:10 (w:v) soil dry weight:solution) on a TOC- V_{CHS} analyzer (Shimadzu, Kyoto, Japan).

Microbial biomass C and N

Microbial biomass C and N were measured with a chloroform slurry extraction (Fierer 2003).

Subsamples of 10 g of field-moist soil were shaken in 40 mL 0.5 M K_2SO_4 with or without addition of 0.5 mL chloroform. Chloroform was purged from the extracts with room air for 30 minutes. Extracts were filtered (0.9 μm pore size) and analyzed for organic C and N on a TOC- V_{CHS} analyzer coupled with a TNM-1 Total nitrogen measuring unit (Shimadzu, Kyoto, Japan).

Microbial biomass C and N were calculated as the difference in organic C or N between subsamples extracted with chloroform and subsamples extracted without chloroform (Brookes et

al., 1985; Vance et al., 1987). No correction factor for extraction efficiency was used and thus I report a “flush” in microbial biomass C after extraction with chloroform.

Soil hydrolytic enzyme activities

Potential extracellular soil enzyme activities (see Table 3 for their function) were measured with fluorogenic substrates (Marx et al., 2001). The following enzymes were measured with the respective substrates: (i) α -glucosidase (AG) with 4-methylumbelliferyl- α -D-glucopyranoside; (ii) 1,4- β -cellobiohydrolase (CBH) with 4-MUF- β -D-cellobioside (iii); β -glucosidase (BG) with 4-methylumbelliferyl β -D-glucopyranoside; (iv) N-acetyl- β -D-glucosaminidase (NAG) with 4-methylumbelliferyl N-acetyl- β -D-glucosaminide; and (v) L-Leucine aminopeptidase (LAP) with L-Leucine-7-amido-4-methylcoumarin. Substrates -iv were dissolved in 0.4% methylcellosolve. All substrates were prepared at 1 mM (200 μ M final assay concentration) and kept at -20 °C until use. Soil slurries were prepared in modified universal buffer adjusted to pH 6.5 (1:100 (w:v) soil dry weight:solution) by blending for 1 min and subsequently stirring on a magnetic stirrer. Assays were performed in black 96-well microtiter plates by mixing 50 μ L of substrate with 200 μ L of soil slurry. Separate calibration curves were prepared for each soil by mixing 200 μ L of soil slurry with 50 μ L of 4-methylumbelliferone (MU) (for substrates -iv) or 7-amino-4-methylcoumarin (AMC) (for substrate v) standard at different concentrations. Plates were incubated in the dark at room temperature. Fluorescence intensity was determined at 360 nm excitation and 460 nm emission wavelength on an Infinite M Nano+ plate reader (Tecan, Männedorf, Switzerland) at 5 different timepoints over a 2-3 h period. Calibration curves were used to transform fluorescence units into nmol MU or AMC released. Enzyme activities were calculated as the slope of nmol MU or AMC release over time. All enzyme activities are expressed as nmol MU or AMC released g^{-1} soil dry weight min^{-1} .

Table 3. Soil extracellular enzymes measured and their abbreviations and functions.

| Enzyme | Abbreviation | Function |
|--|--------------|-----------------------|
| α-glucosidase | AG | Starch degradation |
| 1,4-β-cellobiohydrolase | CBH | Cellulose degradation |
| β-glucosidase | BG | Cellulose degradation |
| N-acetyl-β-D-glucosaminidase | NAG | Chitin degradation |
| L-Leucine aminopeptidase | LAP | Peptide breakdown |

Soil organic matter fractionation

Soil organic matter was fractionated into POC, sand-associated organic C and silt and clay-associated organic C using a combination of density and size fractionation modified from Soong & Cotrufo (2015). We separated MAOC into a sand fraction and a silt and clay fraction because they vary in turnover time and the silt and clay fraction is thought to be much more important in determining C stabilization (Poeplau et al. 2018). Therefore, from now on I will only consider the silt and clay fraction as MAOC. Briefly, 5g of oven-dried soil was dispersed in 1.65 g cm⁻³ sodium poly-tungstate (SPT) by applying 200 J mL⁻¹ ultrasonic energy at 60 W. After centrifugation (2500 g for 60 min), the floating light fraction (representing POC) was aspirated and collected on a 0.45 μ m glass fiber filter using a vacuum-filtration unit and rinsed with nanopure water. The heavy fraction pellet was washed with nanopure water and passed through a 53 μ m sieve to separate the sand fraction (>53 μ m) from the silt and clay fraction (<53 μ m). All fractions were oven-dried (60°C), weighed and then finely ground. The ground fractions were analyzed for % C and % N on a FlashEA 1112 NC analyzer (Thermo Fisher Scientific Inc., Waltham, MA). Weight recovery was 100% \pm 1% (mean \pm standard deviation) and C and N recoveries were 108% \pm 14% and 106% \pm 17%, respectively.

Carbon stabilization efficiency

I measured C stabilization efficiency (CSE) as the amounts of ^{13}C -glucose additions that were retained in soil versus $^{13}\text{CO}_2$ respired in short (24 h) and long (2 weeks) incubations. Since glucose is typically completely taken up by microbes within a few hours after addition, the ^{13}C retained in soils is expected to represent ^{13}C in microbial biomass and ^{13}C in microbially-produced residues which may contribute to long-term C storage in soils (Geyer et al., 2020). The short incubation represents community-scale CSE (=CSE_C) and is thought to closely track the efficiency of the microbial community to incorporate C in microbial products. The long incubation represents ecosystem-scale CSE (=CSE_E) and integrates CSE_C and the recycling of microbial necromass and residues, and is thus affected by soil organo-mineral interactions (Geyer et al., 2016). I chose 24h for CSE_C as it is a widely used incubation time for short incubations facilitating comparisons with other studies. I chose 2 weeks for CSE_E because preliminary tests showed that the CO₂ pulse after label addition was largely over after 2 weeks, and thus no significant further partitioning of ^{13}C between soil and atmosphere is expected after that point (Geyer et al., 2020).

To reduce costs and logistical challenges, I measured CSE only on beneath shrub samples during the wet season. Due to higher microbial densities, the microbial pump and effects of CSE should be more important in beneath shrub samples (Sokol and Bradford 2019). Three subsamples of 25g air-dried soil per soil sample were weighed into specimen cups (one for CSE_C, one for CSE_E, and one as a natural abundance control). Subsamples were covered with parafilm and pre-incubated at 50% water holding capacity (WHC) and room temperature for 4 days. Label solution of 5 at% ^{13}C -glucose was produced by mixing 99 at% uniformly labelled ^{13}C -glucose with unlabelled glucose in nanopure water. The CSE_C and CSE_E subsamples received label solution that added 27 μg glucose-C g⁻¹ dry soil (~10% of microbial biomass C) and were brought to 60%

WHC. Control subsamples received nanopure water instead of label solution. Specimen cups were immediately sealed into mason jars (473 mL) fitted with rubber septa and flushed with CO₂-free air for 1 minute. All subsamples were incubated at room temperature. After 24 h, CSE_C and control subsamples were destructively harvested. Briefly, a 25 mL headspace gas sample was taken with a syringe and stored in evacuated Exetainers (12 mL). Jars were then opened and 20g of soil was immediately extracted for microbial biomass (data not reported here). The remaining soil was placed in plastic bags and frozen at -20°C. Soil samples were freeze-dried, finely ground and analyzed for % C and ¹³C at % using an EA-IRMS setup consisting of a ECS 4010 Elemental Combustion System (Costech Analytical Technologies Inc., Valencia, CA) coupled to a Delta V Advantage Isotope Ratio Mass Spectrometer via a ConFlo IV (both Thermo Fisher Scientific Inc., Waltham, MA). Gas samples were analyzed for ¹²CO₂ concentration and its isotopic signature by injecting 10 mL of sample into a Picarro Small Sample Injection Module (SSIM) coupled to a Picarro Cavity Ringdown Spectrometer G2201- (Picarro, Santa Clara, CA). Subsamples for CSE_E were incubated for 2 weeks and then harvested in the same way. Representative gas samples were taken after sealing CSE_E subsamples in mason jars during the following 4 timepoints into the incubation: i) 0-24 h, ii) 24-72 h, iii) 5-7 days and iv) 12-14 days. Specimen cups were covered with parafilm when they were not sealed in mason jars.

Calculations and statistical analyses

I calculated CSE using the methods described by Geyer et al. (2020) and the following equations:

$$CSE = \frac{{}^{13}\text{Soil } C}{{}^{13}\text{Soil } C + {}^{13}\text{CO}_2}$$

$${}^{13}\text{Soil } C = {}^{12}\text{Soil } C \times \frac{\text{at}\% \text{ Soil } C_L - \text{at}\% \text{ Soil } C_N}{\text{at}\% \text{ label} - \text{at}\% \text{ Soil } C_N}$$

$${}^{13}\text{CO}_2 = \text{cumulative } {}^{12}\text{CO}_2 \times \frac{\text{at}\% \text{ CO}_{2L} - \text{at}\% \text{ CO}_{2N}}{\text{at}\% \text{ label} - \text{at}\% \text{ CO}_{2N}}$$

where $^{12}\text{Soil C}$ = the total C of soil samples ($\mu\text{g C g}^{-1}$ dry soil), at\% Soil C_L = the at% of labelled samples, at\% Soil C_N = the at% of control samples, at\% label = the at% of the label solution (=5 at %), and $\text{Cumulative } ^{12}\text{CO}_2$ = the cumulative CO_2 respiration over the incubation period as $\mu\text{g CO}_2\text{-C g}^{-1}$ dry soil. Respiration data was blank-corrected using empty mason jars that were flushed with CO_2 -free air and incubated in parallel with soil samples. $^{13}\text{CO}_2$ in the 2-week incubation was calculated as the sum of $^{13}\text{CO}_2$ calculated at the 4 points of gas sampling, with timepoint 1, 2, 3 and 4 representing day 0-1, day 1-4, day 4-8 and day 8-14 of the incubation, respectively.

In CHAP and CSS1, I tested for significant N-fertilization treatment effects using two-way ANOVAs with treatment and soil position (beneath shrub vs. interspace) as fixed factors and plot as random factor. If a significant ($p < 0.05$) or marginally significant ($p < 0.1$) treatment effect was found, I used paired t-tests as post-hoc tests to test for treatment effects within each soil position. P-values in the post-hoc tests were Bonferroni-corrected to account for an increase in type-1 error due to multiple comparisons. I checked for normal distribution of the tested variables using Bartlett tests after standardizing and pooling data points from both treatments and soil positions. Variance homogeneity was evaluated by comparing standard deviations visually. If assumptions were not met, data was log-transformed, square root-transformed, or multiplicative inverse-transformed, in that order. Since I only took samples from beneath shrubs at GRASS and CSS2, I directly compared control and N-fertilized plots in paired t-tests. I checked for normal distribution of the tested variables using Bartlett tests after standardizing and pooling data points from both treatments. If assumptions were not met, data was log-transformed, square root-transformed, or multiplicative inverse-transformed, in that order. I treated control and N-fertilized plots as dependent due to the paired plot design at our sites. This allows us to account for landscape-scale variation in soil and plant properties, significantly improving the statistical power at the low

sample sizes typical for long-term ecosystem studies. I only tested for treatment effects within each site and not across sites, since each site differs in multiple factors such as fertilizer type, acidification, vegetation system and site.

I also used Pearson correlations to explore relationships between POC, MAOC and CSE_C and other soil properties like soil pH, exchangeable Ca, microbial biomass C and dissolved inorganic N. I tested for normal distribution of the tested variables using Bartlett tests. If normal distribution was not fulfilled, variables were log-transformed, square root-transformed, or multiplicative inverse-transformed, in that order. If data was still not normally distributed after transformation, or clear outliers were present, I performed Spearman correlations instead. Results of the correlation analyses are presented in Supp. Table 2. All statistical analyses were performed in R-Studio version 4.1.2 (R Core Team).

RESULTS

Soil organic C fractions

To analyze how N fertilization affected CHAP and CSS1, I first tested for a treatment effect *across* both soil positions (i.e., interspaces together with beneath shrubs) in a two-way ANOVA, and then tested for a N enrichment treatment effect *within* each soil position using paired t-tests (e.g., N fertilized interspaces vs. control interspaces). Since there are no interspace soils for GRASS and CSS2, I tested for a treatment effect at these sites using only paired t-tests.

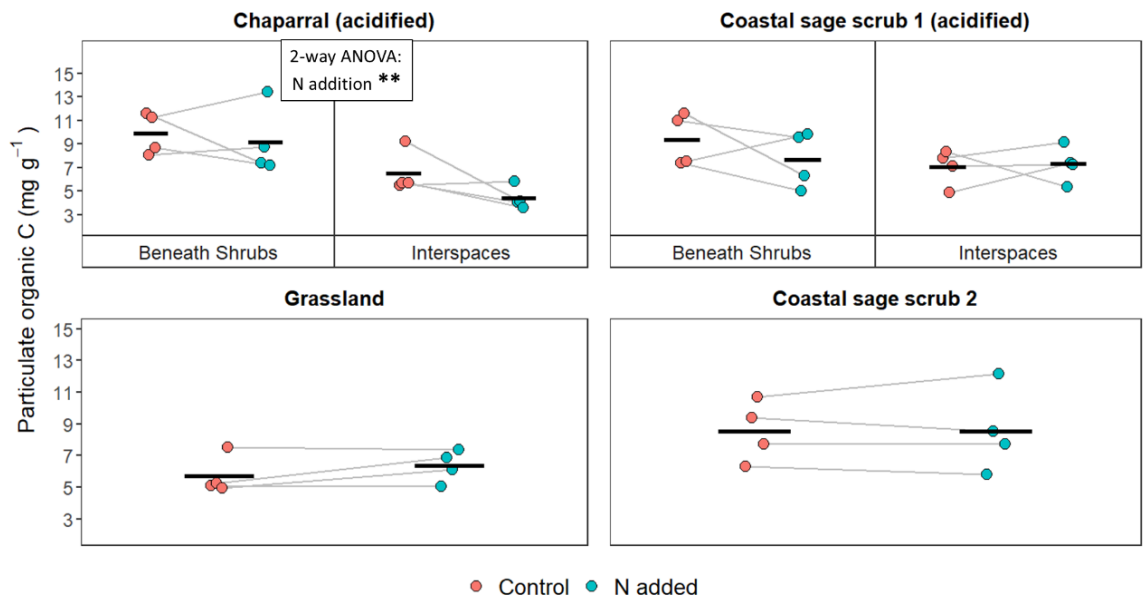


Figure 2. Differences in particulate organic C between control plots and plots fertilized with N during the wet season 2021 in soils from four long-term (> 10 years) N fertilization experiments in Southern California. At Chaparral and Coastal sage scrub 1 soils are from beneath shrubs and from interspaces between shrubs and at Grassland and Coastal sage scrub 2 soils are from beneath vegetation only. Chaparral and Coastal sage scrub 1 experienced strong acidification in response to N fertilization. Dots represent individual data points (4 plots per treatment and soil position) with grey lines connecting paired control and N-fertilized plots. Black crossbars represent means (n=4). If present, significant N fertilization effects across the beneath shrub and interspace samples are given in inset box (two-way ANOVA), and significant N fertilization effects within soil positions (paired t-test) are indicated by symbols above data points (*, p<0.1, **, p<0.05).

Nitrogen fertilization decreased both POC (Fig. 2, $p = 0.024$) and MAOC (Fig. 3, $p = 0.026$) at the acidified CHAP site; across both soil positions (beneath shrubs and in the interspaces between shrubs), POC decreased by 17% and MAOC decreased by 21%. For POC there was a marginally significant interaction between treatment and soil position ($p = 0.091$); the interspaces had a significantly lower POC ($p < 0.001$) than soils beneath shrubs and appeared to decrease more in POC with N addition than soils beneath shrubs. However, no significant treatment effects were found within each soil position using paired t-tests (Fig. 2). Nitrogen fertilization had no effect on SOC fractions at the other sites, including the acidified CSS1 site. Noticeably, at the acidified

sites CHAP and CSS1, 13 out of the 16 samples from N fertilized plots decreased in MAOC while only 9 out of 16 decreased in POC.

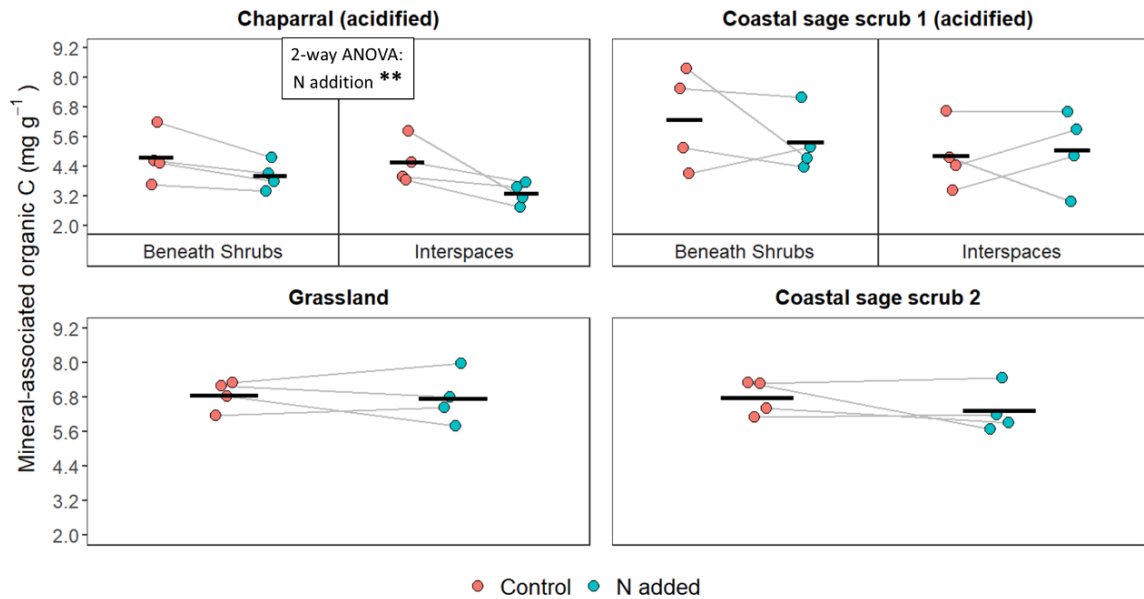


Figure 3. Differences in mineral-associated organic C between control plots and plots fertilized with N during the wet season 2021 in soils from four long-term (> 10 years) N fertilization experiments in Southern California. At Chaparral and Coastal sage scrub 1 soils are from beneath shrubs and from interspaces between shrubs and at Grassland and Coastal sage scrub 2 soils are from beneath vegetation only. Chaparral and Coastal sage scrub 1 experienced strong acidification in response to N fertilization. Dots represent individual data points (4 plots per treatment and soil position) with grey lines connecting paired control and N-fertilized plots. Black crossbars represent means (n=4). If present, significant N fertilization effects across beneath shrub and interspace samples are given in inset box (Two-way ANOVA), and significant N fertilization effects within soil positions (paired t-test) are indicated by symbols above data points (*, p<0.1, **, p<0.05).

Microbial biomass and potential extracellular enzyme activities

N fertilization decreased microbial biomass C by 38% at the acidified CHAP site (Fig. 4, p = 0.009) and by 45% at the acidified CSS1 site (Fig. 4, p = 0.013), but had no effect on microbial biomass C at other sites. At CHAP, microbial biomass C was significantly lower in the interspaces than beneath shrubs (p = 0.001) and, within soil positions, only interspaces marginally

decreased in response to N fertilization ($p = 0.063$). Within soil positions at CSS1, only beneath shrub samples showed a marginally significant decrease in microbial biomass C ($p = 0.092$).

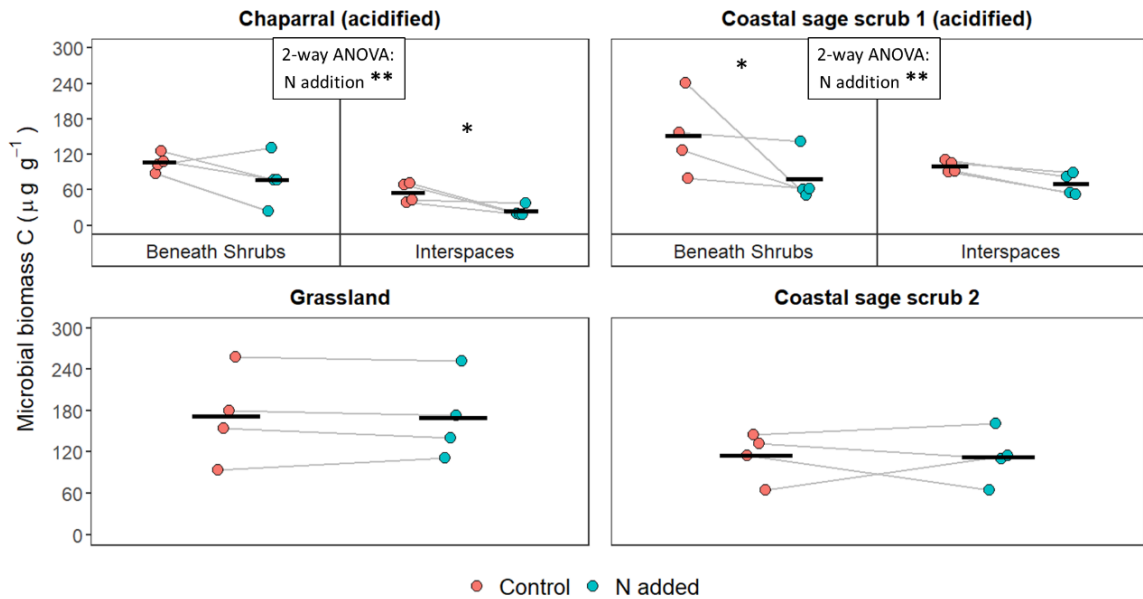


Figure 4. Differences in microbial biomass C between control plots and plots fertilized with N during the wet season 2021 in soils from four long-term (> 10 years) N fertilization experiments in Southern California. At Chaparral and Coastal sage scrub 1 soils are from beneath shrubs and from interspaces between shrubs and at Grassland and Coastal sage scrub 2 soils are from beneath vegetation only. Chaparral and Coastal sage scrub 1 experienced strong acidification in response to N fertilization only. Dots represent individual data points (4 plots per treatment and soil position) with grey lines connecting paired control and N-fertilized plots. Black crossbars represent means ($n=4$). If present, significant N fertilization effects across soil position (beneath shrub and interspace) samples are given in inset box (two-way ANOVA), and significant N fertilization effects within soil positions (paired t-test) are indicated by symbols above data points (*, $p < 0.1$, **, $p < 0.05$).

Potential activities of all C- and N-acquiring extracellular enzymes decreased significantly with N fertilization at the acidified CHAP and CSS1 sites (Table 4), except for N-acquiring NAG which remained unchanged at CSS1. At CHAP, AG decreased by 44% ($p = 0.005$), BG by 64% ($p = 0.001$), CBH by 56% ($p = 0.011$), NAG by 61% ($p = 0.005$) and LAP by 65% ($p < 0.001$). At CSS1, AG decreased by 49% ($p < 0.001$), BG by 52% ($p < 0.001$), CBH by 54% ($p = 0.002$) and LAP by 50% ($p < 0.001$). Furthermore, potential activities of all enzymes were marginally or

significantly lower in interspaces. When I expressed enzyme activity on a per mg microbial biomass basis, N fertilization did not affect enzyme activities except for an increase in NAG at CSS1 (Supp. Table 1). In contrast to the acidified sites, N fertilization had no effect on potential soil cellular enzyme activities at the non-acidified sites GRASS and CSS2 (Table 4).

Table 4. Potential activities of C-acquiring soil extracellular enzymes alpha-glucosidase (AG), beta-glucosidase (BG) and cellobiohydrolase (CBH) and N-acquiring soil extracellular enzymes N-acetylglucosaminidase (NAG) and leucine-aminopeptidase (LAP). Data are means (standard deviation). Numbers in bold indicate significant differences between control plots and plots fertilized with N evaluated in a two-way ANOVA across soil positions for CHAP and CSS1 and in paired t-tests for GRASS and CSS2 ($p < 0.1$).

| | | AG (nmol g ⁻¹ h ⁻¹) | | BG (nmol g ⁻¹ h ⁻¹) | | CBH (nmol g ⁻¹ h ⁻¹) | | NAG (nmol g ⁻¹ h ⁻¹) | | LAP (nmol g ⁻¹ h ⁻¹) | |
|-------|------------|--|------------------------------|--|---------------------------------|---|------------------------------|---|-------------------------------|---|--------------------------------|
| | | Control | N added | Control | N added | Control | N added | Control | N added | Control | N added |
| CHAP | Shrub | 7.80 (1.58) | 3.96 (1.34) | 259.46 (118.92) | 98.71 (24.65) | 17.35 (8.67) | 6.73 (2.35) | 63.96 (26.90) | 26.99 (9.38) | 73.38 (20.45) | 25.49 (3.84) |
| | Interspace | 4.72 (1.31) | 3.02 (1.32) | 81.07 (32.20) | 25.38 (15.37) | 4.73 (1.33) | 3.05 (1.10) | 29.68 (17.83) | 9.20 (2.62) | 41.18 (9.71) | 13.83 (2.40) |
| CSS1 | Shrub | 8.96 (1.22) | 4.26 (1.59) | 332.02 (162.66) | 108.53 (30.26) | 24.25 (7.00) | 9.74 (3.81) | 80.19 (18.41) | 64.48 (8.93) | 121.69 (23.23) | 49.98 (20.99) |
| | Interspace | 6.53 (2.09) | 3.35 (1.12) | 123.17 (26.73) | 75.16 (14.03) | 9.77 (3.61) | 5.32 (1.23) | 46.87 (11.37) | 70.03 (13.15) | 73.40 (12.97) | 48.86 (6.59) |
| GRASS | | 8.36 (2.55) | 7.01 (0.81) | 203.98 (53.90) | 162.27 (49.35) | 20.28 (7.49) | 18.2 (6.20) | 57.90 (20.40) | 62.68 (11.10) | 99.83 (23.89) | 102.73 (14.08) |
| CSS2 | | 10.16 (1.42) | 9.13 (1.80) | 306.57 (35.82) | 282.84 (73.44) | 33.43 (8.45) | 36.31 (12.62) | 94.58 (6.28) | 98.71 (16.69) | 128.48 (5.76) | 133.85 (24.09) |

Carbon stabilization efficiency and exchangeable Ca

Since I measured CSE only in soils sampled beneath shrubs, I tested for an effect of N fertilization on CSE only using paired t-tests. Community-scale CSE (CSE_C), evaluated in the short-term incubations, decreased in all eight N fertilization plots at CHAP and CSS1, but the difference was not significant at CHAP and marginally significant at CSS1 (Fig. 5, $p = 0.095$). In contrast to CSE, N fertilization had no effect on ecosystem-scale CSE (CSE_E), which was evaluated in long-term incubations (Fig. 5). No effects were detected at GRASS and CSS2.

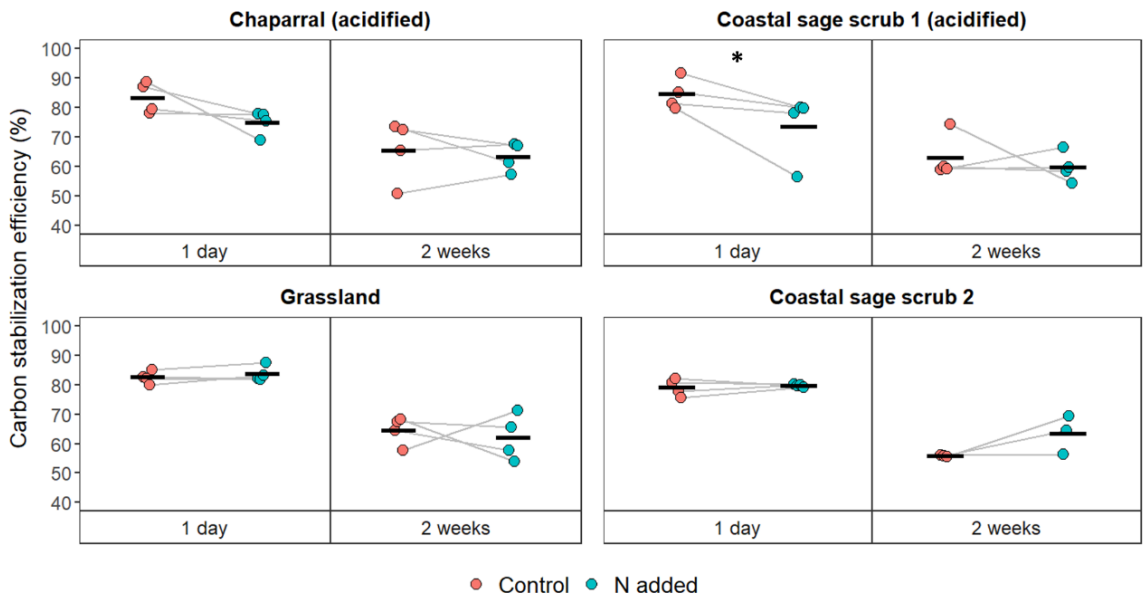


Figure 5. Differences in carbon stabilization efficiency measured in short- (1 day; i.e. community-scale carbon stabilization efficiency (CSE_c)) and long-term (2 weeks; i.e. ecosystem-scale carbon stabilization efficiency (CSE_E)) incubations between control plots and plots fertilized with N during the wet season 2021 in soils from four long-term (> 10 years) N fertilization experiments in Southern California. Chaparral and Coastal sage scrub 1 experienced strong acidification in response to N fertilization. Dots represent individual data points (4 plots per treatment and soil position) with grey lines connecting paired control and N-fertilized plots. Black crossbars represent means ($n=4$). If present, significant N fertilization effects within each incubation time (paired t-test) are indicated by symbols above data points (*, $p<0.1$, **, $p<0.05$).

Long-term N fertilization reduced soil exchangeable Ca at acidified sites; exchangeable Ca decreased by 49% at CHAP (Fig. 6, $p = 0.003$) and by 27% at CSS1 (Fig. 6, $p = 0.011$) when analyzed across samples beneath shrubs and in the interspaces. Within soil positions at CHAP, beneath shrub samples decreased marginally ($p = 0.068$) and interspaces showed no significant decrease according to paired t-tests. There were no treatment effects within soil positions at CSS1 according to paired t-tests. In contrast to the acidified sites, sites fertilized with $CaNO_3$ did not see a decrease in exchangeable Ca; exchangeable Ca increased by 11% at GRASS (Fig. 6, $p = 0.042$) and did not change at CSS2.

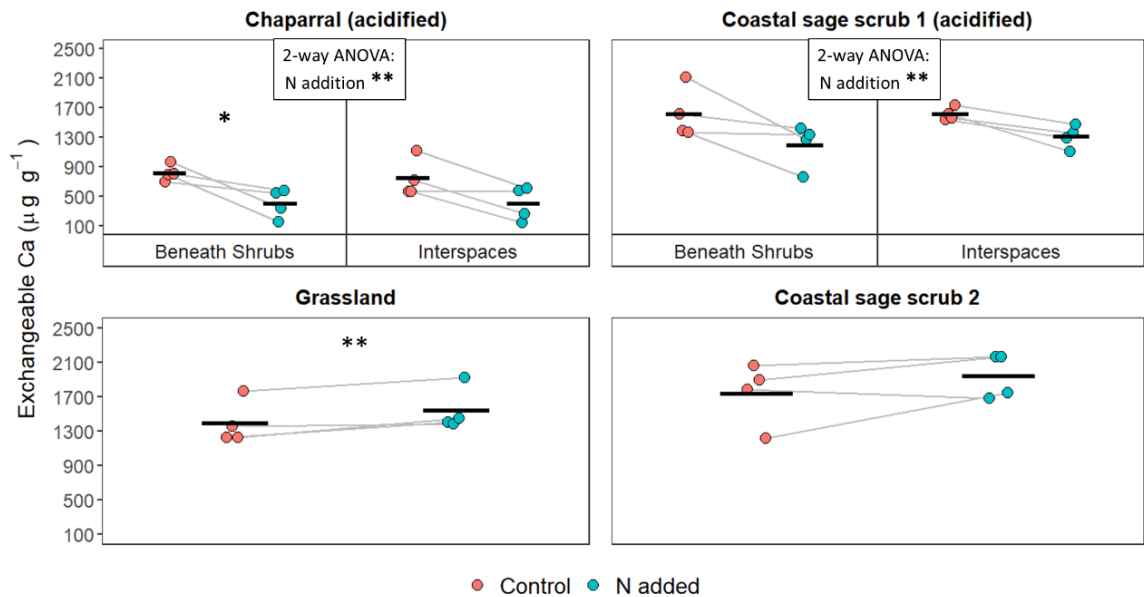


Figure 6. Differences in exchangeable Ca between control plots and plots fertilized with N during the wet season 2021 in soils from four long-term (> 10 years) N fertilization experiments in Southern California. At Chaparral and Coastal sage scrub 1 soils are from beneath shrubs and from interspaces between shrubs and at Grassland and Coastal sage scrub 2 soils are from beneath vegetation only. Chaparral and Coastal sage scrub 1 experienced strong acidification in response to N fertilization. Dots represent individual data points (4 plots per treatment and soil position) with grey lines connecting paired control and N-fertilized plots. Black crossbars represent means (n=4). If present, significant N fertilization effects across beneath shrub and interspace samples are given in inset box (two-way ANOVA), and significant N fertilization effects within soil positions (paired t-test) are indicated by symbols above data points (*, p<0.1, **, p<0.05).

DISCUSSION

I found that long-term experimental N deposition at several dryland sites had relatively small effects on soil organic carbon storage, which appeared to be mostly driven by soil physicochemical changes. Contrary to previous studies, I found no increases in POC despite previously reported increases in above-ground biomass in three of the four study systems (Parolari et al. 2012; Vourlitis et al. 2021a), and likely decreases in biotic decomposition in the two sites that experienced strong acidification as supported by reduced microbial biomass and extracellular enzyme activities. Furthermore, I found no evidence for a microbial carbon pump governing the persistence of soil C under N enrichment; short-term CSE even decreased in the

acidified N plots at CHAP and CSS1 but did not lead to changes in long-term CSE. Importantly, however, I observed significant losses of MAOC at the acidified CHAP site, likely as result of pH-induced Ca loss. Our measurements suggest that long-term effects of N fertilization on dryland C storage might be of abiotic nature, such that in drylands where Ca-stabilization of SOC is prevalent and may undergo acidification may be most at risk for significant loss of MAOC.

Particulate organic C dynamics

Despite reported increases in above-ground biomass at CHAP, CSS1 and GRASS (data for CSS2 are not available) with N enrichment (Parolari et al. 2012; Vourlitis et al. 2021), POC did not increase at either site and even decreased at CHAP during the wet season. In contrast to my findings, N fertilization increased biomass production and POC in other studies in semi-arid grasslands (Ye et al. 2018; Lin et al. 2019). While I did not measure soil respiration, it is unlikely that higher biotic organic matter decomposition offset the increased plant inputs in our study. For example, although litter quality was increased (Allison et al. 2013), litter decomposition did not respond strongly to N addition at GRASS (Allison et al. 2013). Furthermore, N fertilization is predicted to stimulate microbial decomposition only if pH remains more or less constant (Averill and Waring 2018). CHAP and CSS1 experienced strong acidification and a decrease in microbial biomass and hydrolytic extracellular enzyme activities. Soil extracellular enzymes catalyze the breakdown of large organic molecules into smaller C compounds and nutrients and are a major player in organic matter decomposition in soils (Burns et al. 2013). The strong decrease in microbial biomass and almost all hydrolytic enzyme activities suggests that microbial organic matter decomposition is suppressed in acidified sites, which should lead to an increase in POC, such as observed in many mesic ecosystems (Treseder 2008; Zak et al. 2019). Therefore, other processes are likely responsible for preventing POC build-up.

While biotic decomposition likely did not change in non-acidified sites and even decreased in acidified sites, it is possible that abiotic decomposition prevented a build-up of POC from aboveground litter. For example, decomposition increased at a N fertilized and acidified dryland site and was linked to increases in soil Mn (Hou et al. 2021b). Soil Mn is involved in abiotic organic matter degradation and can contribute significantly to the apparent oxidative enzyme activity measured in commonly used enzyme assays (Sanchez-Julia and Turner 2021). Even though I didn't measure changes in soil Mn, a previously reported increase in peroxidase activity at CHAP could hint at a Mn-induced increase in abiotic lignin degradation in response to acidification (Vourlitis et al. 2021b). Furthermore, most of the aboveground litter in drylands can degrade photochemically, independent of litter and soil properties (Berenstecher et al. 2021). Photodegradation may prevent the transfer of aboveground litter into soil as POC and lead to root biomass as the main long-term contributor of POC in dryland soils (Berenstecher et al. 2021). Indeed, a fertilization study in a semi-arid grassland that found increases in POC also reported increases in root biomass (Ye et al. 2018), whereas cumulative root production was unchanged after the first 15 years of fertilization at CHAP and CSS1 (Vourlitis et al. 2021a). Overall, it is possible that abiotic decomposition can decouple increases in above-ground biomass from POC build-up in soil.

It is also possible that POC did not increase because the effects of N fertilization may be masked by annual changes in plant biomass production and decomposition in response to precipitation. Precipitation strongly affects plant biomass production and its response to N addition in drylands (Yahdjian et al. 2011; Hou et al. 2021a), with several studies showing N fertilization only increased plant production under experimental water addition (Ma et al. 2020) or in years of above-average precipitation (Hall et al. 2011; Ladwig et al. 2012; Vourlitis 2012; Su et al. 2013). Similarly, dryland soils can show high seasonal and year-to-year variation in SOC (Hou et al.

2021a). The strong seasonal changes I observed in POC from the dry to the wet season (+47% for POC and only -5% for MAOC, Supp. Fig. 2 and Supp. Fig. 3) suggest that much of the seasonal variation in SOC (+13% in our study, Supp. Fig. 1) observed in drylands is driven by changes in POC, which is considered as a more dynamic pool relative to MAOC (Lavallee et al. 2020). Therefore, seasonal changes might make it challenging to detect differences in POC and, by extension, in SOC. For example, I only found decreases in POC and SOC at CHAP in 2021 but not in 2020, while another study found increases in SOC at CSS2 where I found no changes (Khalili et al. 2016). Similarly, SOC at CHAP and CSS1 responded negatively, positively, or not at all to N fertilization depending on the year of measurement (Vourlitis et al. 2021b). Overall, even if differences in POC may have been detected in some years, the observed dynamic nature of POC suggests that much of the POC in our study may turnover quickly, with only a small fraction contributing to long-term C storage.

Microbial C stabilization efficiency

I found no evidence (i.e., changes in CSE or MAOC) for an acceleration of the microbial C pump under N fertilization in the non-acidified sites at GRASS and CSS2. It has been suggested that if pH stays constant and soils have a high enough sorption potential, then N fertilization should alleviate microbial N limitation, increasing microbial CUE and, thereby, increasing MAOC (Manzoni et al. 2012b; Averill and Waring 2018; Poeplau et al. 2019). The lack of a response measured in CSE or MAOC to N addition could indicate that, in drylands, microbes may be mostly limited by water and C availability (Schaeffer et al. 2003; Homyak et al. 2018; Schimel 2018). For example, low moisture negated the positive relationship between microbial diversity and CUE in a model study (Domeignoz-Horta et al. 2020). Alternatively, microbial CUE can also change in response to changes in microbial community composition (Li et al. 2021). While microbial community composition changed at GRASS (Amend et al. 2016), the changes may not

have been directed enough to favor microbes with a higher CSE (Pold et al. 2020). Overall, I found no evidence that N fertilization increased dryland C storage through changes in microbial CSE.

It is possible I did not detect an acceleration of the microbial C pump under N fertilization because the low sorption potential of soils at our sites inhibits the microbial in-vivo pathway of C stabilization. For example, short-term CSE decreased in all N deposition plots at CHAP and CSS1 but had no effect on long-term CSE. Short-term CSE is mostly affected by microbial community responses while long-term CSE also includes effects of organo-mineral interactions (Geyer et al. 2016). The correlation between pH and CSE_C (Supp. Table 2) indicates that microbial community changes in response to acidification could have accounted for the decrease in short-term CSE at CHAP and CSS1 (Lauber et al. 2009; Jones et al. 2019). However, the fact that the initial differences in CSE did not translate into long-term stabilization means that the additional C that was initially retained in control plots was later recycled over the course of the long-term incubation (Geyer et al. 2016, 2020). Similar to a previous study on low-sorption, sandy soils (Creamer et al. 2014), this could indicate that the C stabilization potential in the studied soils is too low, so that even if microbes initially retain C more efficiently, there is no viable mechanism for long-term storage—the soils may be operating at or near their capacity to store C. Therefore, it is unlikely that N addition would affect C stabilization at our site via the microbial pump and it appears that microbial C accumulation efficiency may strongly depend on soil mineralogy (Cai et al. 2022).

Mineral-associated organic C

I found significant losses of MAOC in response to N fertilization at CHAP during both the end of the dry season and the wet season. At the end of the dry season MAOC was 13% lower in N fertilization plots compared to control plots (Supp. Fig. 3) and during the wet season MAOC was

21% lower in N fertilization plots. Losses of MAOC in drylands have been observed before and linked to increased decomposition (Lin et al. 2019) and acidification (Ye et al. 2018). However, an increase in decomposition rates at our site is unlikely since biotic decomposition likely decreased at CHAP as discussed for POC and potential photodegradation and oxidative degradation should only affect aboveground litter and POC. Furthermore, the fact that the decrease in MAOC was highest in the interspaces between shrubs, which had a significantly lower microbial biomass, points to acidification as the likely driver behind MAOC decrease. Acidification can decrease MAOC by destabilizing Ca-OC associations. Polyvalent cations such as Ca are important in bridging negatively charged C compounds to negatively charged mineral surfaces, particularly in dryland soils (Rasmussen et al. 2018; Rowley et al. 2018). Even though I did not measure Ca-OM pools directly, exchangeable Ca was strongly correlated with MAOC and significantly decreased at CHAP (Fig. 6), suggesting that Ca loss is the main pathway for MAOC decrease at our sites. Our findings are consistent with other studies that reported losses in Ca-associated organic matter in response to N-induced acidification (Ye et al. 2018; Wan et al. 2021). Based on my data, I cannot fully exclude that the observed decrease in MAOC was due to a decrease in microbial C inputs—MAOC was strongly correlated to microbial biomass, which decreased at CHAP. However, assuming that MAOC at our sites is at steady-state, decreased microbial C inputs due to a lower microbial biomass should not destabilize MAOC, since lower microbial biomass would also likely decrease the odds microbes can access and break down MAOC (Jilling et al. 2018; Bailey et al. 2019). Furthermore, it is unlikely that the microbial MAOC formation plays a substantial role in the interspaces between shrubs where microbial biomass was already low and where I found the strongest changes in MAOC (Sokol and Bradford 2019). Overall, my findings suggest that MAOC loss in our study is primarily related to pH-induced destabilization of Ca-OC associations.

While a loss of Ca-associated organic matter can explain the loss of MAOC at our CHAP site, I found that strong acidification and loss of exchangeable Ca did not decrease MAOC at CSS1. On average CSS1 lost less Ca than CHAP (22% vs. 48%) and had higher baseline Ca levels (1616 $\mu\text{g g}^{-1}$ at CSS1 averaged across soil positions in control plots vs. 777 $\mu\text{g g}^{-1}$ at CHAP), perhaps suggesting that there is a threshold beyond which decreases in exchangeable Ca lead to the destabilization of cation bridges and Ca-associated organic matter. However, I found that out of the 16 studied N addition cases at CHAP and CSS1 that experienced acidification and Ca loss, only 3 did not decrease in MAOC. These 3 cases come from two plots at CSS1 which experienced significant dieback of original shrub vegetation and replacement by invasive forbs (George Vourlitis, personal communication). It is possible that a change to a faster cycling grass- and forb-dominated vegetation system with higher root biomass and turnover overrode potential Ca-related C losses and led to C accumulation in these plots (Qi et al. 2019; Sokol and Bradford 2019). Strong increases in SOC upon CSS invasion by grasses have been observed before (Wolkovich et al. 2010). Since N enrichment is expected to shift plant community composition (Plaza et al. 2018a), particularly in CSS (Kimball et al. 2014; Valliere et al. 2017), future studies on how effects of vegetation change on SOC fractions might interact with direct effects of N addition are warranted.

Implications for N deposition effects on C storage in drylands

Given the high seasonal fluctuation in SOS and POC in drylands (this study; Hou et al. 2021a; Vourlitis et al. 2021b), the consistently observed MAOC losses could be the first sign for a future decrease in C storage in dryland sites prone to acidification. Acidification and base cation loss due to N deposition is a global phenomenon and increases with N deposition rate (Tian and Niu 2015). Therefore, high N deposition areas around urban centers and agricultural hotspots should be most at risk for acidification (Fenn et al. 2010), especially if the soils are not well buffered.

Furthermore, the form of N deposited, either as NH_4^+ or NO_3^- , can affect soil acidification (Tian and Niu 2015). While NH_3 emission can initially buffer acidity in precipitation, once deposited, NH_4^+ can still cause acidification depending on how much of it is taken up by plants and how much of it is nitrified (Rodhe et al. 2002). Notably, nitrification produces 2 H^+ ions and NO_3^- , which can then co-leach from the system as a companion anion to base cations (Rodhe et al. 2002). Therefore, the partitioning between NO_3^- leaching, transformation of NO_3^- to gaseous by-products, and plant NO_3^- uptake might also be important in determining acidification and base cation loss potential. Since a global shift from NO_3^- to NH_3 deposition is expected (Lamarque et al. 2013; Kanakidou et al. 2016), future studies should focus specifically on how the deposition and consumption pathways of these compounds affect acidification in drylands.

Even if acidification occurs, C losses should mostly be limited to topsoils in areas in which Ca-associations make up an important portion of C stabilization. While there is currently no good understanding of the distribution of Ca-associated organic C pools, correlation studies suggest that Ca should be particularly important in C stabilization in drylands above pH 6.5 and dominated by 2:1 phyllosilicates (Rasmussen et al. 2018). Even if these sites acidify, it seems like Ca loss may be mostly constrained to the first 10 cm of the soil profile (Niu et al. 2021), although data is limited. Since most of the C in soils is stored below 10 cm (Dynarski et al. 2020), the impact of pH-induced C loss for the global C budget should be limited if only topsoil is affected. However, C decreases in topsoil could still have important future consequences for soil structure, water holding capacity and soil fertility in the drylands affected. Notably, changes in POC from above-ground biomass might not help to balance out these losses if above-ground litter is prevented from building up in soils (Berenstecher et al. 2021), particularly since root biomass doesn't always increase in response to N enrichment (Kummerow et al. 1982; Ladwig et al. 2012; Vourlitis et al. 2021a).

REFERENCES

- Allison SD, Lu Y, Weihe C, et al (2013) Microbial abundance and composition influence litter decomposition response to environmental change. *Ecology* 94:714–725. doi: 10.1890/12-1243.1
- Amend AS, Martiny AC, Allison SD, et al (2016) Microbial response to simulated global change is phylogenetically conserved and linked with functional potential. *ISME Journal* 10:109–118. doi: 10.1038/ismej.2015.96
- Averill C, Waring B (2018) Nitrogen limitation of decomposition and decay: How can it occur? *Global Change Biology* 24:1417–1427. doi: 10.1111/gcb.13980
- Bailey VL, Pries CH, Lajtha K (2019) What do we know about soil carbon destabilization? *Environmental Research Letters* 14:083004
- Berenstecher P, Araujo PI, Austin AT (2021) Worlds apart: Location above- or below-ground determines plant litter decomposition in a semi-arid Patagonian steppe. *Journal of Ecology* 109:2885–2896. doi: 10.1111/1365-2745.13688
- Bradford MA, Keiser AD, Davies CA, et al (2013) Empirical evidence that soil carbon formation from plant inputs is positively related to microbial growth. *Biogeochemistry* 113:271–281. doi: 10.1007/s10533-012-9822-0
- Brookes PC, Landman A, Pruden G, Jenkinson DS (1985) Chloroform fumigation and the release of soil nitrogen: A rapid direct extraction method to measure microbial biomass nitrogen in soil. *Soil Biology and Biochemistry* 17:837–842. doi: 10.1159/000477898
- Burns RG, DeForest JL, Marxsen J, et al (2013) Soil enzymes in a changing environment: Current knowledge and future directions. *Soil Biology and Biochemistry* 58:216–234. doi: 10.1016/j.soilbio.2012.11.009
- Butcher KR, Nasto MK, Norton JM, Stark JM (2020) Physical mechanisms for soil moisture effects on microbial carbon-use efficiency in a sandy loam soil in the western United States. *Soil Biology and Biochemistry* 150:107969. doi: 10.1016/j.soilbio.2020.107969
- Cai Y, Ma T, Wang Y, et al (2022) Assessing the accumulation efficiency of various microbial carbon components in soils of different minerals. *Geoderma* 407:115562. doi: 10.1016/j.geoderma.2021.115562
- Castellano MJ, Mueller KE, Olk DC, et al (2015) Integrating plant litter quality, soil organic matter stabilization, and the carbon saturation concept. *Global Change Biology* 21:3200–3209. doi: 10.1111/gcb.12982
- Cotrufo MF, Ranalli MG, Haddix ML, et al (2019) Soil carbon storage informed by particulate

- and mineral-associated organic matter. *Nature Geoscience* 12:989–994. doi: 10.1038/s41561-019-0484-6
- Creamer CA, Jones DL, Baldock JA, et al (2016) Is the fate of glucose-derived carbon more strongly driven by nutrient availability, soil texture, or microbial biomass size? *Soil Biology and Biochemistry* 103:201–212. doi: 10.1016/j.soilbio.2016.08.025
- Creamer CA, Jones DL, Baldock JA, Farrell M (2014) Stoichiometric controls upon low molecular weight carbon decomposition. *Soil Biology and Biochemistry* 79:50–56. doi: 10.1016/j.soilbio.2014.08.019
- Deng L, Huang C, Shangguan DKZ, et al (2020) Soil GHG fluxes are altered by N deposition : New data indicate lower N stimulation of the N₂O flux and greater stimulation of the calculated C pools. *Global Change Biology* 26:2613–2629. doi: 10.1111/gcb.14970
- Domeignoz-Horta LA, Pold G, Liu XJA, et al (2020) Microbial diversity drives carbon use efficiency in a model soil. *Nature Communications* 11:3684. doi: 10.1038/s41467-020-17502-z
- Dynarski KA, Bossio DA, Scow KM (2020) Dynamic Stability of Soil Carbon: Reassessing the “Permanence” of Soil Carbon Sequestration. *Frontiers in Environmental Science* 8:514701. doi: 10.3389/fenvs.2020.514701
- Fenn ME, Allen EB, Weiss SB, et al (2010) Nitrogen critical loads and management alternatives for N-impacted ecosystems in California. *Journal of Environmental Management* 91:2404–2423. doi: 10.1016/j.jenvman.2010.07.034
- Fierer N (2003) *Stress ecology and the dynamics of microbial communities and processes in soil.* ProQuest Dissertations Publishing, University of California, Santa Barbara
- Geyer K, Schnecker J, Grandy AS, et al (2020) Assessing microbial residues in soil as a potential carbon sink and moderator of carbon use efficiency. *Biogeochemistry* 4:237–249. doi: 10.1007/s10533-020-00720-4
- Geyer KM, Kyker-snowman E, Grandy AS, Frey SD (2016) Microbial carbon use efficiency: accounting for population, community, and ecosystem-scale controls over the fate of metabolized organic matter. *Biogeochemistry* 127:173–188. doi: 10.1007/s10533-016-0191-y
- Gruber N, Galloway JN (2008) An Earth-system perspective of the global nitrogen cycle. *Nature* 451:293–296. doi: 10.1038/nature06592
- Hall SJ, Sponseller RA, Grimm NB, et al (2011) Ecosystem response to nutrient enrichment across an urban airshed in the Sonoran Desert. *Ecological Applications* 21:640–660. doi: 10.1890/10-0758.1
- Harpole SW, Potts DL, Suding KN (2007) Ecosystem responses to water and nitrogen amendment in a California grassland. *Global Change Biology* 13:2341–2348. doi:

10.1111/j.1365-2486.2007.01447.x

- Hendershot WH, Duquette M (1986) A simple barium chloride method for determining cation exchange capacity and exchangeable cations. *Soil Science Society of America Journal* 50:605–608. doi: 10.2136/sssaj1986.03615995005000030013x
- Homyak PM, Blankinship JC, Slessarev EW, et al (2018) Effects of altered dry season length and plant inputs on soluble soil carbon. *Ecology* 99:2348–2362. doi: 10.1002/ecy.2473
- Homyak PM, Sickman JO, Miller AE, et al (2014) Assessing Nitrogen-Saturation in a Seasonally Dry Chaparral Watershed: Limitations of Traditional Indicators of N-Saturation. *Ecosystems* 17:1286–1305. doi: 10.1007/s10021-014-9792-2
- Hou E, Rudgers JA, Collins SL, et al (2021a) Sensitivity of soil organic matter to climate and fire in a desert grassland. *Biogeochemistry* 156:59–74. doi: 10.1007/s10533-020-00713-3
- Hou SL, Hättenschwiler S, Yang JJ, et al (2021b) Increasing rates of long-term nitrogen deposition consistently increased litter decomposition in a semi-arid grassland. *New Phytologist* 229:296–307. doi: 10.1111/nph.16854
- Janssens IA, Dieleman W, Luyssaert S, et al (2010) Reduction of forest soil respiration in response to nitrogen deposition. *Nature Geoscience* 3:315–322. doi: 10.1038/ngeo844
- Jilling A, Keiluweit M, Contosta AR, et al (2018) Minerals in the rhizosphere: overlooked mediators of soil nitrogen availability to plants and microbes. *Biogeochemistry* 139:103–122. doi: 10.1007/s10533-018-0459-5
- Jones DL, Cooledge EC, Hoyle FC, et al (2019) pH and exchangeable aluminum are major regulators of microbial energy flow and carbon use efficiency in soil microbial communities. *Soil Biology and Biochemistry* 138:107584. doi: 10.1016/j.soilbio.2019.107584
- Kanakidou M, Myriokefalitakis S, Daskalakis N, et al (2016) Past, present, and future atmospheric nitrogen deposition. *Journal of the Atmospheric Sciences* 73:2039–2047. doi: 10.1175/JAS-D-15-0278.1
- Khalili B, Ogunseitan OA, Goulden ML, Allison SD (2016) Interactive effects of precipitation manipulation and nitrogen addition on soil properties in California grassland and shrubland. *Applied Soil Ecology* 107:144–153. doi: 10.1016/j.apsoil.2016.05.018
- Kimball S, Goulden ML, Suding KN, Parker S (2014) Altered water and nitrogen input shifts succession in a southern California coastal sage community. *Ecological Applications* 24:1390–1404. doi: 10.1890/13-1313.1
- Kummerow J, Avila G, Aljaro M-E, et al (1982) Effect of fertilizer on fine root density and shoot growth in Chilean matorral. *Botanical Gazette* 143:498–504
- Ladwig LM, Collins SL, Swann AL, et al (2012) Above- and belowground responses to nitrogen

- addition in a Chihuahuan Desert grassland. *Oecologia* 169:177–185. doi: 10.1007/s00442-011-2173-z
- Lamarque JF, Dentener F, McConnell J, et al (2013) Multi-model mean nitrogen and sulfur deposition from the atmospheric chemistry and climate model intercomparison project (ACCMIP): Evaluation of historical and projected future changes. *Atmospheric Chemistry and Physics* 13:7997–8018. doi: 10.5194/acp-13-7997-2013
- Lauber CL, Hamady M, Knight R, Fierer N (2009) Pyrosequencing-based assessment of soil pH as a predictor of soil bacterial community structure at the continental scale. *Applied and Environmental Microbiology* 75:5111–5120. doi: 10.1128/AEM.00335-09
- Lavallee JM, Soong JL, Cotrufo MF (2020) Conceptualizing soil organic matter into particulate and mineral - associated forms to address global change in the 21st century. *Global Change Biology* 26:261–273. doi: 10.1111/gcb.14859
- Li J, Sang C, Yang J, et al (2021) Stoichiometric imbalance and microbial community regulate microbial elements use efficiencies under nitrogen addition. *Soil Biology and Biochemistry* 156:108207. doi: 10.1016/j.soilbio.2021.108207
- Liang C, Schimel JP, Jastrow JD (2017) The importance of anabolism in microbial control over soil carbon storage. *Nature Microbiology* 2:17105. doi: 10.1038/nmicrobiol.2017.105
- Lin Y, Slessarev EW, Yehl ST, et al (2019) Long-term nutrient fertilization increased soil carbon storage in California grasslands. *Ecosystems* 22:754–766. doi: 10.1007/s10021-018-0300-y
- Ma Q, Liu X, Li Y, et al (2020) Nitrogen deposition magnifies the sensitivity of desert steppe plant communities to large changes in precipitation. *Journal of Ecology* 108:598–610. doi: 10.1111/1365-2745.13264
- Maestre FT, Eldridge DJ, Soliveres S, et al (2016) Structure and Functioning of Dryland Ecosystems in a Changing World. *Annual Review of Ecology, Evolution, and Systematics* 47:215–237. doi: 10.1146/annurev-ecolsys-121415-032311
- Manzoni S, Taylor P, Richter A, et al (2012a) Environmental and stoichiometric controls on microbial carbon-use efficiency in soils. *New Phytologist* 196:79–91. doi: 10.1111/j.1469-8137.2012.04225.x
- Manzoni S, Taylor P, Richter A, et al (2012b) Environmental and stoichiometric controls on microbial carbon-use efficiency in soils. *New Phytologist* 196:79–91. doi: 10.1111/j.1469-8137.2012.04225.x
- Marx M-C, Wood M, Jarvis SC (2001) A microplate fluorimetric assay for the study of enzyme diversity in soils. *Soil Biology and Biochemistry* 33:1633–1640
- Niu G, Wang R, Hasi M, et al (2021) Availability of soil base cations and micronutrients along soil profile after 13-year nitrogen and water addition in a semi-arid grassland. *Biogeochemistry* 152:223–236. doi: 10.1007/s10533-020-00749-5

- O’Sullivan M, Spracklen D V., Batterman SA, et al (2019) Have synergies between nitrogen deposition and atmospheric CO₂ driven the recent enhancement of the terrestrial carbon sink? *Global Biogeochemical Cycles* 33:163–180. doi: 10.1029/2018GB005922
- Ochoa-hueso R, Maestre FT, Ríos ADL, et al (2013) Nitrogen deposition alters nitrogen cycling and reduces soil carbon content in low-productivity semiarid Mediterranean ecosystems. *Environmental Pollution* 179:185–193. doi: 10.1016/j.envpol.2013.03.060
- Parolari AJ, Goulden ML, Bras RL (2012) Fertilization effects on the ecohydrology of a southern California annual grassland. *Geophysical Research Letters* 39:L08405. doi: 10.1029/2012GL051411
- Plaza C, Gascó G, Méndez AM, et al (2018a) *Soil Organic Matter in Dryland Ecosystems*. Elsevier Inc.
- Plaza C, Zaccone C, Sawicka K, et al (2018b) Soil resources and element stocks in drylands to face global issues. *Scientific Reports* 8:13788. doi: 10.1038/s41598-018-32229-0
- Poeplau C, Don A, Six J, et al (2018) Isolating organic carbon fractions with varying turnover rates in temperate agricultural soils – A comprehensive method comparison. *Soil Biology and Biochemistry* 125:10–26. doi: 10.1016/j.soilbio.2018.06.025
- Poeplau C, Helfrich M, Dechow R, et al (2019) Increased microbial anabolism contributes to soil carbon sequestration by mineral fertilization in temperate grasslands. *Soil Biology and Biochemistry* 130:167–176. doi: 10.1016/j.soilbio.2018.12.019
- Pold G, Domeignoz-Horta LA, Morrison EW, et al (2020) Carbon use efficiency and its temperature sensitivity covary in soil bacteria. *mBio* 11:e02293-19. doi: 10.1128/mBio.02293-19
- Potts DL, Suding KN, Winston GC, et al (2012) Ecological effects of experimental drought and prescribed fire in a southern California coastal grassland. *Journal of Arid Environments* 81:59–66. doi: 10.1016/j.jaridenv.2012.01.007
- Právělie R (2016) Drylands extent and environmental issues. A global approach. *Earth-Science Reviews* 161:259–278. doi: 10.1016/j.earscirev.2016.08.003
- Qi Y, Wei W, Chen C, Chen L (2019) Plant root-shoot biomass allocation over diverse biomes: A global synthesis. *Global Ecology and Conservation* 18:e00606. doi: 10.1016/j.gecco.2019.e00606
- Rasmussen C, Heckman K, Wieder WR, et al (2018) Beyond clay : towards an improved set of variables for predicting soil organic matter content. *Biogeochemistry* 137:297–306. doi: 10.1007/s10533-018-0424-3
- Riggs CE, Hobbie SE (2016) Mechanisms driving the soil organic matter decomposition response to nitrogen enrichment in grassland soils. *Soil Biology and Biochemistry* 99:54–65. doi:

10.1016/j.soilbio.2016.04.023

- Rodhe H, Dentener F, Schulz M (2002) The global distribution of acidifying wet deposition. *Environmental Science and Technology* 36:4382–4388. doi: 10.1021/es020057g
- Rossi LMW, Mao Z, Merino-Martín L, et al (2020) Pathways to persistence: plant root traits alter carbon accumulation in different soil carbon pools. *Plant and Soil* 452:457–478. doi: 10.1007/s11104-020-04469-5
- Rowley MC, Grand S, Verrecchia ÉP (2018) Calcium-mediated stabilisation of soil organic carbon. *Biogeochemistry* 137:27–49. doi: 10.1007/s10533-017-0410-1
- Sanchez-Julia M, Turner BL (2021) Abiotic contribution to phenol oxidase activity across a manganese gradient in tropical forest soils. *Biogeochemistry* 153:33–45. doi: 10.1007/s10533-021-00764-0
- Schaeffer SM, Billings SA, Evans RD (2003) Responses of soil nitrogen dynamics in a Mojave Desert ecosystem to manipulations in soil carbon and nitrogen availability. *Oecologia* 134:547–553. doi: 10.1007/s00442-002-1130-2
- Schimel JP (2018) Life in dry soils: Effects of drought on soil microbial communities and processes. *Annual Review of Ecology, Evolution, and Systematics* 49:409–432. doi: 10.1146/annurev-ecolsys-110617-062614
- Slessarev EW, Lin Y, Bingham NL, et al (2016) Water balance creates a threshold in soil pH at the global scale. *Nature* 540:567–569. doi: 10.1038/nature20139
- Sokol NW, Bradford MA (2019) Microbial formation of stable soil carbon is more efficient from belowground than aboveground input. *Nature Geoscience* 12:46–53. doi: 10.1038/s41561-018-0258-6
- Sokol NW, Sanderman J, Bradford MA (2019) Pathways of mineral - associated soil organic matter formation : Integrating the role of plant carbon source , chemistry , and point of entry. *Global Change Biology* 25:12–24. doi: 10.1111/gcb.14482
- Soong JL, Cotrufo MF (2015) Annual burning of a tallgrass prairie inhibits C and N cycling in soil, increasing recalcitrant pyrogenic organic matter storage while reducing N availability. *Global Change Biology* 21:2321–2333. doi: 10.1111/gcb.12832
- Spohn M, Pötsch EM, Eichorst SA, et al (2016) Soil microbial carbon use efficiency and biomass turnover in a long-term fertilization experiment in a temperate grassland. *Soil Biology and Biochemistry* 97:168–175. doi: 10.1016/j.soilbio.2016.03.008
- Su J, Li X, Li X, Feng L (2013) Effects of additional N on herbaceous species of desertified steppe in arid regions of China: A four-year field study. *Ecological Research* 28:21–28. doi: 10.1007/s11284-012-0994-9
- Tian D, Niu S (2015) A global analysis of soil acidification caused by nitrogen addition.

- Environmental Research Letters 10:024019. doi: 10.1088/1748-9326/10/2/024019
- Treseder KK (2008) Nitrogen additions and microbial biomass: A meta-analysis of ecosystem studies. *Ecology Letters* 11:1111–1120. doi: 10.1111/j.1461-0248.2008.01230.x
- Valliere JM, Irvine IC, Santiago L, Allen EB (2017) High N , dry : Experimental nitrogen deposition exacerbates native shrub loss and nonnative plant invasion during extreme drought. *Global Change Biology* 23:4333–4345. doi: 10.1111/gcb.13694
- Vance ED, Brookes PC, Jenkinson DS (1987) An extraction method for measuring soil microbial biomass C. *Soil Biology and Biochemistry* 19:703–707. doi: 10.1016/0038-0717(87)90052-6
- Vourlitis GL (2012) Aboveground net primary production response of semi-arid shrublands to chronic experimental dry-season N input. *Ecosphere* 3:Article 22
- Vourlitis GL, Jauregui J, Marin L, Rodriguez C (2021a) Shoot and root biomass production in semi-arid shrublands exposed to long-term experimental N input. *Science of the Total Environment* 754:142204. doi: 10.1016/j.scitotenv.2020.142204
- Vourlitis GL, Kirby K, Vallejo I, et al (2021b) Potential soil extracellular enzyme activity is altered by long-term experimental nitrogen deposition in semiarid shrublands. *Applied Soil Ecology* 158:103779. doi: 10.1016/j.apsoil.2020.103779
- Wan D, Ma M, Peng N, et al (2021) Effects of long-term fertilization on calcium-associated soil organic carbon: Implications for C sequestration in agricultural soils. *Science of the Total Environment* 772:145037. doi: 10.1016/j.scitotenv.2021.145037
- Weil RR, Brady NC (2017) *The Nature and Properties of Soils*, 15th edn. Pearson Education Limited, Essex, England
- Wolkovich EM, Lipson DA, Virginia RA, et al (2010) Grass invasion causes rapid increases in ecosystem carbon and nitrogen storage in a semiarid shrubland. *Global Change Biology* 16:1351–1365. doi: 10.1111/j.1365-2486.2009.02001.x
- Xu C, Xu X, Ju C, et al (2021) Long-term, amplified responses of soil organic carbon to nitrogen addition worldwide. *Global Change Biology* 27:1170–1180. doi: 10.1111/gcb.15489
- Yahdjian L, Gherardi L, Sala OE (2011) Nitrogen limitation in arid-subhumid ecosystems: A meta-analysis of fertilization studies. *Journal of Arid Environments* 75:675–680. doi: 10.1016/j.jaridenv.2011.03.003
- Ye C, Chen D, Hall SJ, et al (2018) Reconciling multiple impacts of nitrogen enrichment on soil carbon: plant, microbial and geochemical controls. *Ecology Letters* 21:1162–1173. doi: 10.1111/ele.13083

Zak DR, Argiroff WA, Freedman ZB, et al (2019) Anthropogenic N deposition, fungal gene expression, and an increasing soil carbon sink in the Northern Hemisphere. *Ecology* 100:e02804. doi: 10.1002/ecy.2804